HAL
open science

Classical percolation fingerprints in the high-temperature regime of the integer quantum Hall effect

Martina Flöser, B. A. Piot, C. L. Campbell, Duncan Kennedy Maude, M. Henini, R. Airey, Z. R. Wasilewski, Serge Florens, T. Champel

To cite this version:

Martina Flöser, B. A. Piot, C. L. Campbell, Duncan Kennedy Maude, M. Henini, et al.. Classical percolation fingerprints in the high-temperature regime of the integer quantum Hall effect. New Journal of Physics, 2013, 15, pp.083027. 10.1088/1367-2630/15/8/083027 . hal-00855299

HAL Id: hal-00855299

https://hal.science/hal-00855299v1

Submitted on 16 Mar 2022

HAL is a multi-disciplinary open access archive for the deposit and dissemination of scientific research documents, whether they are published or not. The documents may come from teaching and research institutions in France or abroad, or from public or private research centers.

L'archive ouverte pluridisciplinaire **HAL**, est destinée au dépôt et à la diffusion de documents scientifiques de niveau recherche, publiés ou non, émanant des établissements d'enseignement et de recherche français ou étrangers, des laboratoires publics ou privés.

arXiv:1212.2031v2 [cond-mat.mes-hall] 22 Aug 2013

Classical percolation fingerprints in the high temperature regime of quantum Hall effect

M. Flöser[1], B. A. Piot[2], C. L. Campbell[2], D. K. Maude[2], M. Henini[3], R. Airey[4], Z. R. Wasilewski[5], S. Florens[1], T. Champel[6]

[1] Institut Néel, CNRS and Université Joseph Fourier, B.P. 166, 25 Avenue des Martyrs, F-38042 Grenoble, France

[2] Laboratoire National des Champs Magnétiques Intenses, CNRS, UJF-UPS-INSA, F-38042 Grenoble, France

[3] School of Physics and Astronomy, University of Nottingham, Nottingham NG7 2RD, United Kingdom

[4] Department of Electronic and Electrical Engineering, University of Sheffield, Sheffield S1 4DU, United Kingdom

[5]Department of Electrical and Computer Engineering University of Waterloo, Waterloo, ON, Canada

[6] Laboratoire de Physique et Modélisation des Milieux Condensés, CNRS and Université Joseph Fourier, B.P. 166, F-38042 Grenoble, France

Abstract. We have performed magnetotransport experiments in the high-temperature regime (up to 50 K) of the integer quantum Hall effect for two-dimensional electron gases in semiconducting heterostructures. While the magnetic field dependence of the classical Hall law presents no anomaly at high temperatures, we find a breakdown of the Drude-Lorentz law for the longitudinal conductance beyond a crossover magnetic field $B_c \simeq 1$ T, which turns out to be correlated with the onset of the integer quantum Hall effect at low temperatures. We show that the high magnetic field regime at $B > B_c$ can be understood in terms of classical percolative transport in a smooth disordered potential. From the temperature dependence of the peak longitudinal conductance, we extract scaling exponents which are in good agreement with the theoretically expected values. We also prove that inelastic scattering on phonons is responsible for dissipation in a wide temperature range going from 1 to 50 K at high magnetic fields.

PACS numbers: 73.43.-f,72.15.Rn,64.60.ah

1. Introduction

Two-dimensional electron gases (2DEGs) under perpendicular magnetic fields have revealed at low temperatures a wealth of surprising transport properties [1, 2, 3], which are direct manifestations of quantum mechanics at the macroscopic scale. Remarkably, in the same 2DEG system one may observe gradually by increasing the magnitude of the magnetic field B different quantum phenomena [4]: Shubnikov-de Haas (SdH) oscillations, followed by integer and then fractional quantum Hall effects (QHE). All these effects capitalize on the quantization of the cyclotron orbital motion resulting from the Lorentz force, which gives rise to discrete kinetic energy levels $E_n = (n + 1/2)\hbar\omega_c$ (with n a positive integer, $\omega_c = |e|B/m^*$ the cyclotron frequency, $e = -|e|$ the electron charge, m^* the effective mass, and $\hbar$ Planck's constant divided by 2π). The QHE characterized by a spectacularly robust quantization of the Hall conductance in integral [1] or fractional [2] multiples of e^2/h differ from the SdH (diffusive) regime by the quasi-absence of dissipation in the bulk, as vindicated by the spectacular drop in magnitude of the longitudinal conductance minima. This transition is usually understood with the onset of a quasi-ballistic transport regime [5], associated with the localization of all the bulk states except at the center of a Landau level [4] where a diffusive electronic propagation throughout the system can set in only via percolation. A semiclassical localization mechanism [6, 7, 8] resulting from the decoupling of the (quantized) cyclotron motion with the guiding center, which leads to a quasi-regular drift of the electronic states along constant energy contours of the smooth disorder potential landscape, has recently been confirmed [9, 10] by scanning tunneling spectroscopy in the integer QHE regime. Percolative spatial structures for the local density of states taking place at the transition between Hall plateaus have also been clearly identified in this local probe experiment [9]. Signatures of percolation in transport properties have been mainly discussed in the literature [11, 12, 13, 14, 15, 16, 17] at very low temperatures (typically below $T = 1$ K), when several quantum mechanical effects (tunneling, quantum coherence, etc...) play a role [18, 19, 20, 21, 22, 23, 24, 25, 26] and complicate the analysis both theoretically and experimentally. However, if the localization mechanism for the QHE is classical in nature, we expect these percolative features at high magnetic fields to be also observable at much higher temperatures, in a classical transport regime.

In this paper, we study the nature of the high magnetic field, high temperature transport regime, combining experimental measurements in the 1-50 K range with recent theoretical predictions [27, 28]. We first identify a crossover magnetic field $B_c \simeq 1$ T above which chaotic classical (diffusive) dynamics breaks down, that we correlate to the onset of QHE at low temperature. This observation points to the common origin of long-range disorder in suppressing the diffusive regime, both in the classical and quantum realms. For $B > B_c$ we observe various scaling laws that demonstrate the combined role of phonon scattering and classical percolation in the transport properties.

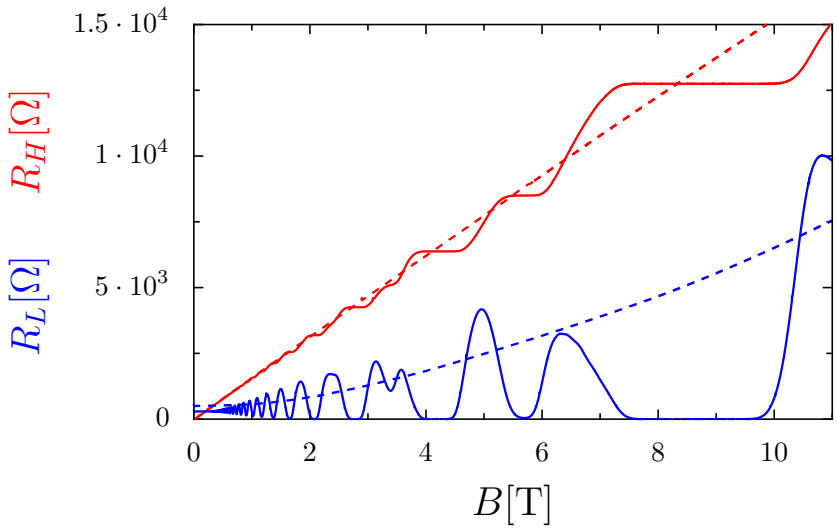

Figure 1. Longitudinal R_L (bottom curves) and Hall R_H (top curves) resistances as a function of magnetic field at $T = 1.2$ K (solid lines) and $T = 47$ K (dashed lines) for sample 1.

2. Observation of a breakdown of Drude-Lorentz law in high magnetic field

The 2DEGs used in our study are delta-doped $Al_xGa_{1-x}As/GaAs$ heterostructures patterned into a Hall bar. The transport measurements were performed with a standard low frequency lock-in technique for temperatures T between 1.2 K and 50 K in a variable temperature insert, under magnetic fields up to 11 T. The first (second) sample has a mobility $\mu_e = 3.3 \cdot 10^5$ cm^2/Vs at 1.2 K ($8 \cdot 10^4$ cm^2/Vs), and an electron density $n_e = 4 \cdot 10^{11}$ cm^{-2} ($7 \cdot 10^{11}$ cm^{-2}). The two samples differ also by their growth process since sample 1 is an heterojunction, while sample 2 is a quantum well [29]. A particular attention has been paid to the mobility range of the samples chosen to investigate the high-temperature regime of the QHE. On the one hand, high enough mobility was required by the need to clearly separate the crossover magnetic field B_c for which the classical localization is expected to set in and the B-scale where the quantization of the cyclotron motion starts to be felt (typically, $B \simeq 0.2$ T corresponds to $\hbar\omega_c \simeq 4k_BT$ for the lowest temperatures studied here). On the other hand, very high mobility samples had to be avoided because of the importance of many-body effects (such as e.g. spin splitting) blurring the physics under consideration.

The B-dependences of the Hall and longitudinal resistances for sample 1 are shown in Fig. 1 at low and high temperatures ($T = 1.2$ K and $T = 47$ K, respectively). The low-T field-dependence is quite standard with the appearance of well-formed plateaus for Hall resistance R_H which are accompanied by strong oscillations of the longitudinal resistance R_L with vanishing minima for fields $B \gtrsim 1$ T. We note that peaks of R_L start to be spin-resolved for $B \geq 3$ T at this low temperature due to the critical many-body enhancement of the spin gap. At high T, R_H becomes structureless and exhibits a linear dependence in field as expected from classical Hall's law. The observed

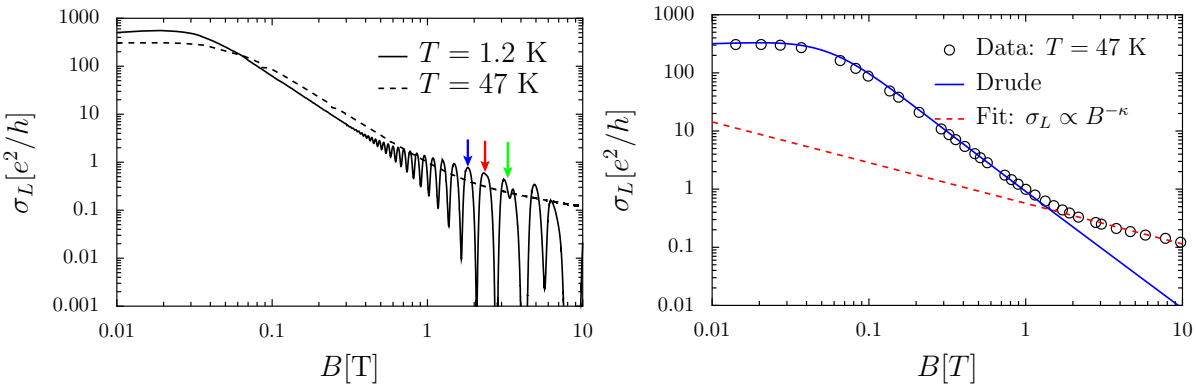

Figure 2. Left panel: Longitudinal magnetoconductance σ_L for sample 1 as a function of magnetic field at $T = 1.2$ K (solid line) and $T = 47$ K (dashed line), correlating the breakdown of mild SdH oscillations in the quantum regime to the one of Drude-Lorentz law in the classical limit. Arrows denote a set of conductance peaks associated to the quantum Hall transitions examined in Fig. 3. Right panel: study of the high temperature data (circles). Drude's law (1) is well obeyed for $B < B_c = 1$ T (top solid line), while an anomalous power law $B^{-\kappa}$ with $\kappa = 0.7 \pm 0.1$ is seen at $B > B_c$ (bottom dashed line).

longitudinal magnetoresistance shows a richer and more instructive field dependence. While R_L saturates according to the classical behavior at low magnetic fields, it shows for $B \gtrsim 1$ T a steady super-linear increase with the magnetic field. A similar positive and slightly non-linear magnetoresistance is found for sample 2, see Appendix.

This transition regime for the longitudinal dissipative transport coefficient is better analyzed in terms of conductance σ_L rather than resistance, see Fig. 2. The magnetic field separating the SdH regime from the integer QHE regime is identified at low T in the range 1-2 T by the exponential drop of σ_L in its minima values. It is interesting to correlate this observation with the measurement performed at high T, especially on a logarithmic scale as shown in Fig. 2. Classically, σ_L is expected to obey the Drude-Lorentz law,

$$\sigma_L = \frac{n_e e^2}{m^*} \frac{\tau_{\rm tr}}{1 + (\omega_c \tau_{\rm tr})^2}, \tag{1}$$

where $\tau_{\rm tr}$ is the transport time determined by the combined scattering on the (random) impurity potential and by phonons. As long as $\omega_c \tau_{\rm tr} \ll 1$, σ_L remains constant, while a quadratic decrease $\sigma_L \propto B^{-2}$ is expected when $\omega_c \tau_{\rm tr} \geq 1$. Drude's law (1), also associated to a constant magnetoresistance R_L in Fig. 1, is well verified up to the magnetic field $B_c \sim 1$ T, with $\tau_{\rm tr} = 7.4 \cdot 10^{-12}$ s at $T = 47$ K. Above B_c, an anomalous power-law dependence, namely $\sigma_L \propto B^{-\kappa}$ with $\kappa \approx 0.7 \pm 0.1$, is revealed by the logarithmic plot of Fig. 2. Interestingly, we note that this breakdown of Drude's law at high T appears correlated to the onset of the QHE at low T. Because we are working at a relatively high T, it is very likely that this breakdown has a purely classical origin.

A linear classical magnetoresistance in several high-mobility samples at high T, qualitatively similar to that shown in Fig. 1, has already been reported several

years ago by Rötger *et al.* [30]. These observations were correlated to the empirical proportionality relation between longitudinal and Hall resistances, $R_L \propto B\,\mathrm{d}R_H/\mathrm{d}B$, originally pointed out in the low temperature quantum Hall regime in Ref. [31]. Indeed, in the classical Hall regime where $R_H \propto B$, this empirical relation predicts a purely linear longitudinal magnetoresistance. It has been argued that this linear behavior at high temperature could be explained by macroscopic density inhomogeneities in the sample [32]. Nevertheless, we note that this interpretation leaves unexplained the clear transition to the constant Drude-Lorentz resistance at low magnetic field as observed in our data, see Fig. 1.

More recent studies by Renard *et al.* [33] evidenced obvious non-linearities in the high T magnetoconductance, with a dependence $R_L \propto B^{\alpha}$ and an exponent $\alpha \simeq 0.9 - 1.1$. This translates into a high-field dependence for the conductance $\sigma_L \propto B^{-\kappa}$, where the exponent $\kappa \approx 0.9$. This turns out to be higher than the value of 0.7 ± 0.1 that we have extracted for sample 1, but all these measurements concur to invalidate both the high-field Drude-Lorentz law $\sigma_L \propto B^{-2}$ and the empirical relation (between R_H and R_L) leading to $\sigma_L \propto B^{-1}$. The appearance of a non-integer exponent κ is rooted in the percolative nature of transport in actual samples, which is the main issue addressed in this paper.

Note that in our other sample 2, we obtain $\kappa \approx 0.8 \pm 0.1$ (see Appendix), i.e., again a non-linearity of the magnetoconductance. The error bars on the high-field scaling exponent κ are mainly due to the limited range of magnetic field which can be used, making a very accurate extraction of κ difficult from a simple field-dependence. Indeed, even at $T = 50$ K, Landau level quantization gives rise to noticeable quantum oscillations of σ_L superposed to the power-law scaling background $\sigma_L \propto B^{-\kappa}$, since $\hbar\omega_c \simeq 4k_BT$ for magnetic field $B > 8$ T.

To understand these discrepancies between the different extracted exponents, it is necessary to better characterize the disorder potential in the different samples. The analysis of the magnetic field dependence of SdH oscillations at temperature $T = 1.2$ K leads to a quantum lifetime $\tau_q = 1.2$ ps for sample 1, and $\tau_q = 0.6$ ps for sample 2. The transport lifetimes calculated at the same temperature from mobility measurements ($\tau_{\mathrm{tr}} = 12.7$ ps in sample 1, and $\tau_{\mathrm{tr}} = 3$ ps in sample 2) are in both samples larger than the quantum lifetimes, what shows the dominant contribution of long range scattering due to a long range disorder potential. The ratio of the transport time to the single-particle scattering time ($\tau_{\mathrm{tr}}/\tau_q = 10.6$ in sample 1, $\tau_{\mathrm{tr}}/\tau_q = 5$ in sample 2) is however not as strong for sample 2, indicating the non negligible contribution of short range scattering mechanisms in the sample (such as, e.g., surface roughness), which could be at the origin of the observed discrepancies. With the help of a theoretical analysis of the data to be developped in the next section, we will first confirm the above exponent values by using in addition the temperature scaling of the magnetoconductance, which will further support the present interpretation for the exponent dispersions.

3. Theoretical analysis of magnetotransport data

A breakdown of law (1) has been predicted in a few theoretical papers [34, 35] addressing long-range disorder at large magnetic field. Essentially, Drude-Lorentz formula relies on classical diffusive transport with chaotic electronic motion due to elastic collisions on impurities at low magnetic fields. When the cyclotron radius becomes basically smaller than the correlation length of the disorder potential, this evolves at high magnetic fields into a quasi-ballistic transport regime with a regular motion of the guiding center along the constant energy contours of the disorder potential landscape, which follows mainly closed trajectories. Macroscopic transport then only takes place by following an extended percolating backbone occurring at a single critical energy and passing through many saddle points of the disorder landscape. The fractal nature of the percolating contour is expected to give rise to non-trivial universal exponents in the temperature and magnetic field dependences of σ_L, as reported here at high magnetic fields. However, it is worth stressing that the percolating contour alone is not sufficient to allow macroscopic transport, since the guiding center drift velocity vanishes at the saddle-points of the disorder landscape. Different microscopic dissipative processes may a priori be at play to provide a finite drift velocity at these transport bottlenecks, an issue that will be clarified in the present work.

It has been argued in Ref. [34], that the high temperature crossover field B_c for the Drude-Lorentz breakdown should be quite close to the low temperature transition between the SdH and QHE regimes. Our experiments in the two samples corroborate this scenario. However, the classical prediction [34] of an exponential suppression of σ_L with B above B_c, which is based on a mechanism of dissipative transport via a stochastic layer around the percolating contour resulting from elastic scattering on the disorder random potential only, is not consistent with the power-law decrease seen in Fig. 2, hinting at more efficient relaxation processes.

We now provide detailed theoretical analysis of our experimental data. The high-B percolative transport regime can be described in terms of a Ohm's law involving a local conductivity tensor [36, 37, 27, 28], which takes the form

$$\hat{\sigma}(\mathbf{r}) = \begin{pmatrix} \sigma_0 & -\sigma_H(\mathbf{r}) \\ \sigma_H(\mathbf{r}) & \sigma_0 \end{pmatrix}, \tag{2}$$

where σ_0 encodes dissipative processes (assumed to be uniform), and $\sigma_H(\mathbf{r})$ is the local Hall component, whose spatial dependence originates from charge density fluctuations due to disorder $V(\mathbf{r})$ in the sample. The local conductivity model expresses the inhomogeneous nature of the high-magnetic field transport, which results from the formation of local equilibrium, and is valid at temperatures high enough so that phase-breaking processes, such as electron-phonon scattering, occur on length scales that are shorter than the typical variations of disorder. The Ohmic conductivity σ_0 is assumed very weak [i.e., $\sigma_0 \ll \sigma_H(\mathbf{r})$] but finite. A priori, it may be due to other scattering mechanisms than elastic impurity scattering such as electron-phonon

scattering [36, 38, 27, 28]. It has been found [37, 27] from model (2) that the longitudinal conductance scales as

$$\sigma_L = C\left[\sigma_0(T,B)\right]^{1-\kappa}\left|\frac{e^2}{h}\sqrt{\langle V^2\rangle}\sum_{n=0}^{\infty} n_F'(E_n-\mu)\right|^{\kappa}, \tag{3}$$

where κ is a non-trivial exponent previously conjectured [37] to be $\kappa = 10/13 \approx 0.77$, a result confirmed recently by a diagrammatic approach [27]. Here C is a nonuniversal dimensionless constant, μ is the chemical potential, and n_F' is the derivative of the Fermi-Dirac distribution function. Formula (3) has been established under the assumption that $\sigma_H(\mathbf{r})$ follows *linearly* the spatial fluctuations of disorder $V(\mathbf{r})$, what requires a sufficiently high T. Typically, it does not describe the low temperature regime [39, 28] when the peak conductance starts to level off around conductance values of the order of $e^2/2h$ (per spin). Another important limitation of formula (3) is the assumption of a Gaussian correlated disorder with a single correlation length, which is valid for impurities located far away from the gas and in absence of sources of short-range impurity scattering. For instance, sample 2 (a quantum well) is likely characterized by multi-scale disorder, which would involve extra (unknown) microscopic parameters in the modelling , making difficult a quantitative comparison to theory (see discussion in Appendix).

In addition, model (2) leads [37, 28] to the conventional classical Hall's law at $T \gg \hbar\omega_c$, where fingerprints of percolations are absent. It predicts therefore a slight breakdown of the empirical proportionality law (between R_L and R_H) due to the non-linearity related to the non-integer exponent κ. Indeed, this gives at high magnetic field $R_L \propto \sigma_L R_H^2 \propto B^{2-\kappa}$, which is non-linear for $\kappa \neq 1$. It has been argued [37] however that the presence of disorder on multiple length scales tends to increase the exponent κ towards 1, thus recovering the empirical proportionality law in the case of more inhomogeneous samples.

Expression (3) yields oscillations of σ_L in B in the percolation regime when $k_BT \leq \hbar\omega_c$, which are superposed on a high-T classical background conductance (obtained for $k_BT > \hbar\omega_c$)

$$\sigma_{\rm bg}(T,B) = C\left[\sigma_0(T,B)\right]^{1-\kappa}\left[\frac{e^2}{h}\frac{\sqrt{\langle V^2\rangle}}{\hbar\omega_c}\right]^{\kappa}. \tag{4}$$

It has been predicted [27] that the peak values for σ_L are given by the formula

$$\sigma_L^{\rm peak} = \sigma_{\rm bg}(T,B)\left[1+\sum_{l=1}^{\infty}\frac{4\pi^2 l k_B T}{\hbar\omega_c}{\rm csch}\left(\frac{2\pi^2 l k_B T}{\hbar\omega_c}\right)\right]^{\kappa}. \tag{5}$$

We deduce from Eq. (4) that in the classical percolative regime σ_L should scale in B as $\sigma_L \propto \left[\sigma_0(T,B)\right]^{1-\kappa} B^{-\kappa}$. Provided that σ_0 is quasi-constant in magnetic field, we find a power-law scaling $\sigma_L \propto B^{-\kappa}$, which globally agrees with the experimental B-dependences reported above.

We now consider the temperature dependence of the conductance in the percolative transport regime, focusing on the spin-unresolved conductance peaks indicated by

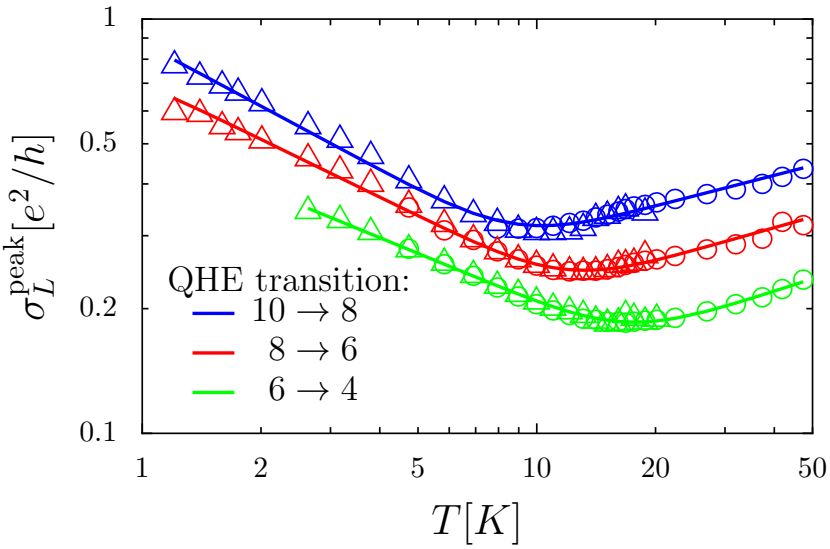

Figure 3. Temperature dependence of the peak longitudinal conductance at the QHE transitions with filling factors $10 \to 8$, $8 \to 6$, and $6 \to 4$ (top to bottom) for sample 1, as indicated by arrows on Fig. 2. Triangles design values measured at the conductance peaks, and circle values taken at fixed B field (see text). The lines are the fit curves with Eq. (5) and the fit parameters given in Table 1.

arrows on Fig. 2. In the low temperature range, we monitor and follow the conductance maxima, which are plotted as triangles on Fig. 3. At higher T, these peaks are washed out and cannot be followed individually anymore, but the magnetic field may be then kept constant, as the conductance becomes weakly field-dependent (circles on Fig. 3). We also note that the opening of the spin gap at the highest magnetic fields considered here limits the temperature range where Zeeman and many body effects can be neglected. We first observe on Fig. 3 the presence of a pronounced minimum at a temperature that perfectly correlates for each peak with the scale $T^* = \hbar\omega_c/(4k_B)$ where quantized Landau levels start to emerge, a striking effect that went previously unnoticed to our knowledge. In addition, two different power-law scalings (with a negative power at $T < T^*$ and positive one at $T > T^*$) are clearly seen, that we would like to attribute to the critical state associated to classical percolation. It can be easily noted from Fig. 3 that the classical conductance seems to scale as $\sigma_L \propto T^{1-\kappa}$ for $T > T^*$, what implies a linear temperature dependence for σ_0 according to Eq. (4).

In order to understand this rich temperature dependence of the conductance peaks, we now need to characterize microscopically the missing piece in formulas (4)-(5), namely the dissipative contribution σ_0. Its origin may be the inelastic electrons-phonons scattering, as has been put forward in many theoretical papers [38, 40, 41]. If we assume that the electrons undergo a large number of scattering events on the phonons, i.e., their rate $\tau_{\rm ph}^{-1}$ is much higher than the characteristic frequency of drift motion, we can estimate the *short-distance* dissipative conductivity σ_0 using the Drude-Lorentz formula

$$\sigma_0 = \frac{n_e e^2}{m^*} \frac{\tau_{\rm ph}}{1 + (\omega_c \tau_{\rm ph})^2}, \tag{6}$$

where $\tau_{\rm ph}$ is the electron-phonon scattering time. Our estimation of $\tau_{\rm ph}$ in the regime of the quantum Hall effect follows that from Ref. [42] using Fermi's golden rule [43]. This yields [42] a scattering rate $\tau_{\rm ph}^{-1} \propto B^2 T$. Inserting this result in Eq. (6), we obtain that σ_0 indeed scales linearly in temperature and is independent of magnetic field whenever $\omega_c \tau_{\rm ph} \gg 1$, vindicating an asumption made earlier. It is worth mentioning that the temperature range where the linear T-dependence of $\tau_{\rm ph}^{-1}$ is valid increases at high magnetic fields [42]. The saturation of $\tau_{\rm ph}^{-1}$ due the spontaneaous phonon emission [45] is expected to take place typically at low temperatures in the Kelvin range, which is beyond the present analysis.

From the established $\sigma_0 \propto T$ law, formulas (3-5) predict that the cyclotron energy separates two distinct physical regimes of transport: i) at $T > T^*$ percolation of guiding centers carrying a classical cyclotron motion occurs, leading to $\sigma_L^{\rm peak} \propto T^{1-\kappa} = T^{3/13}$. This is easily established by noting that the r.h.s. term under brackets in Eq. (5) becomes constant in temperature; ii) at $T < T^*$, the cyclotron motion becomes quantized while the transport of the guiding center remains classical, changing the T-dependence into a *negative* power-law $\sigma_L^{\rm peak} \propto T^{1-2\kappa} = T^{-7/13}$. This new power-law derives directly from Eq. (3), noting that the Fermi function derivative behaves as $1/T$ at low temperature. The assumption of a dissipation mechanism with phonons combined with formula (5) thus not only describe qualitatively our data for the temperature dependence of $\sigma_L^{\rm peak}$, but also provides a very precise way of extracting the classical exponent κ.

The fits performed on Fig. 3 for three successive plateau transitions yield the results given in Table 1. This comparison is performed by considering $\sigma_{\rm bg} = AT^{1-\kappa}$, where the amplitude A and the critical exponent κ are the only fitting parameters. We find that the agreement between the experimental data and the fitting curve is excellent for almost two decades in temperatures. The consistency of the results obtained from both the temperature and magnetic field dependences of σ_L also provides good confidence in the theory. For the peak located at the transition between filling factors 10 to 8 ($B = 1.7$ T), the values extracted for the critical exponent κ are very close to the theoretical prediction $\kappa = 10/13 \simeq 0.77$. We note that the agreement weakens for lower filling factors, where spin splitting effects may play an increasing role that we have not accounted for in the calculation.

B [T]	A [in units of h/e^2 K$^{\kappa-1}$]	κ
1.7	0.16	0.76 ± 0.03
2.3	0.115	0.73 ± 0.03
3.3	0.071	0.70 ± 0.02

Table 1. Fit parameters for Fig. 3.

Turning to sample 2, the analysis of the temperature dependence of each studied conductance peak yields $\kappa \approx 0.85 \pm 0.05$ (for more details, see Appendix), which is consistent with the exponent extracted from the B-dependence. This slightly larger value for the classical percolation exponent in sample 2 could be due to the presence of

disorder fluctuations over different length scales, which have the effect of increasing the effective percolation exponent as discussed in Ref. [37]. Indeed, sample 2 is a narrow (8.2 nm) quantum well, which, in addition to impurity potential, exposes the electron gas to interface roughness.

4. Summary

In conclusion, we have shown that the onset of the quantum Hall effect at low temperatures is directly linked with a breakdown of the classical diffusive regime at high temperatures. We have pointed out that temperature and magnetic field dependences of the longitudinal conductance follow peculiar scaling power-laws in the breakdown regime. We have found a good agreement between theory and experimental data, which confirms that transport is dominated by classical percolation in a wide temperature range going from 1 to 50 K in 2DEGs at high magnetic fields. The analysis also shows that the interaction of phonons with bulk drift states provides the dominant dissipation mechanism at play in this temperature regime.

Acknowledgments

We thank D. Basko and V. Renard for interesting discussions, and ANR "METROGRAPH" under Grant No. ANR-2011-NANO-004-06 for financial support.

Appendix

We present in this appendix the results obtained for sample 2 (quantum well), which has been grown differently from sample 1 (heterojunction). We will follow the logic of the main text, by first considering the magnetic field dependence, and finally the temperature behavior of the longitudinal conductance in the high temperature regime of the quantum Hall effect.

Appendix .1. Magnetic field dependence of transport coefficients in sample 2

In Fig. 1, we present the magnetic field dependences of the Hall and longitudinal resistances observed in sample 2, at temperatures $T = 1.2$ K and 50 K. At low temperatures, the integer quantum Hall effect is clearly observed above magnetic fields $B \gtrsim 2$ T. As reported in Fig. 1, the longitudinal resistance of the second sample also displays a steady increase with the magnetic field for fields $B \gtrsim 2$ T at high temperatures, a behavior which turns out to be again correlated with the onset of the quantum Hall effect at low temperatures. We note that the transition from the Shubnikov-de Haas regime to the quantum Hall regime occurs at a slightly higher crossover field than in sample 1. This observation is consistent with the fact that the mobility in sample 2 is smaller than in sample 1 (which is likely characterized by a smoother disorder potential landscape).

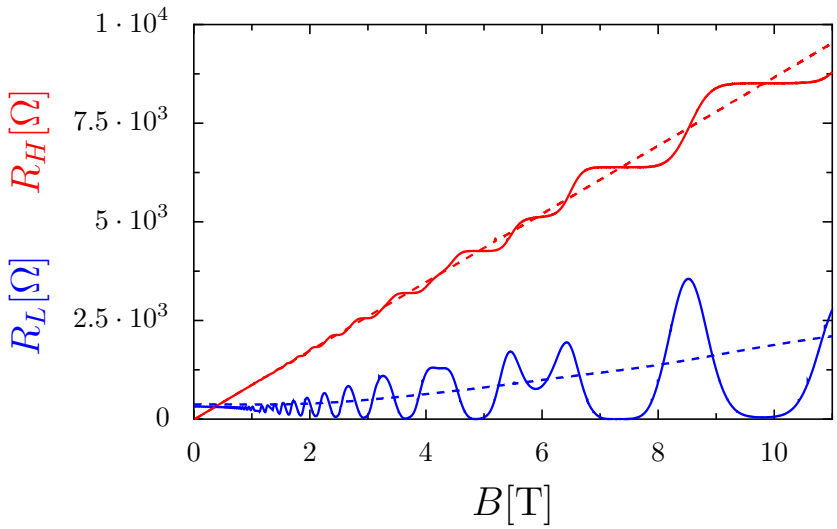

Figure 1. Longitudinal R_L (bottom curves) and Hall R_H (top curves) resistances as a function of magnetic field at $T = 1.2$ K (solid lines) and $T = 50$ K (dashed lines) for sample 2.

The B-dependence of the longitudinal transport coefficient can be better analyzed quantitatively in terms of conductance in a logarithmic scale, as shown in Fig. 2. The Drude-Lorentz law Eq. (1) perfectly describes the low-field part of the conductance and yields $\tau_{\rm tr} = 2.85 \cdot 10^{-12}$ s at $T = 50$ K. At higher magnetic fields $B \gtrsim 2$ T, the Drude-lorentz law also clearly breaks down in sample 2, with the scaling dependence $\sigma_L \propto B^{-\kappa}$ and $\kappa \approx 0.8$.

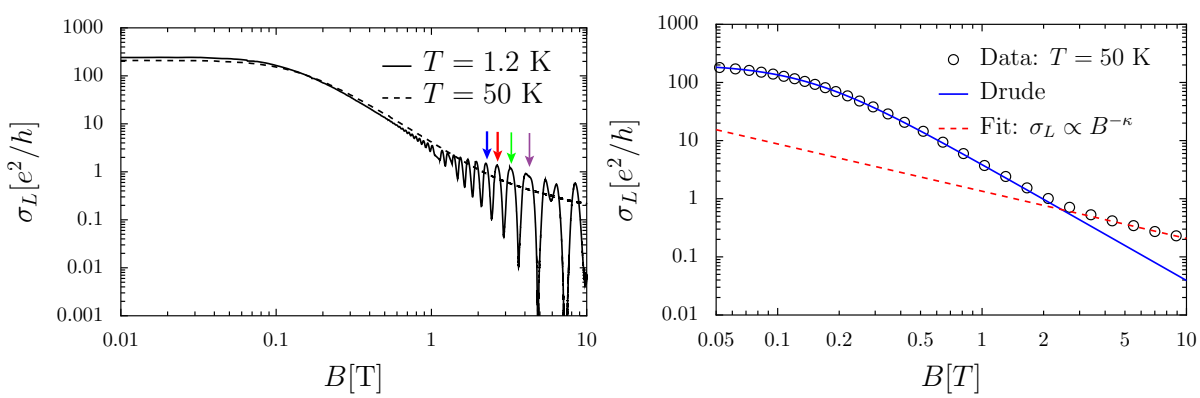

Figure 2. Left panel: Longitudinal magnetoconductance σ_L for sample 2 as a function of magnetic field at $T = 1.2$ K (solid line) and $T = 50$ K (dashed line), correlating the breakdown of mild SdH oscillations in the quantum regime to the one of Drude's law in the classical limit. Arrows denote a set of conductance peaks associated to the quantum Hall transitions examined in Fig. 3. Right panel: study of the high temperature data (circles). Drude law Eq. (1) is well obeyed for $B < B_c = 2$ T (top solid line), while an anomalous power law $B^{-\kappa}$ with $\kappa = 0.8 \pm 0.1$ is seen at $B > B_c$ (bottom solid line) for the studied sample.

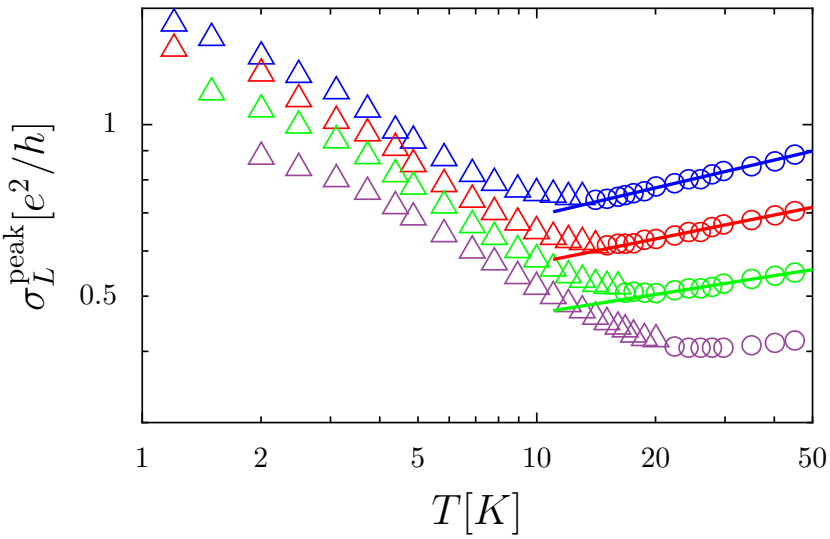

Figure 3. Temperature dependence of the peak longitudinal conductance for sample 2. The selected peaks are indicated by arrows on Fig. 2. Triangles design values measured at the conductance peaks, and circle values taken at fixed B field. The lines are fit to $\sigma_L = AT^{1-\kappa}$, with parameters given in Table 1. The lower curve (for $B = 4.28$ T) cannot be reliably fitted due to the reduced range in temperature.

Appendix .2. Temperature dependence of the peak longitudinal conductance in sample 2

As discussed in the main text, a more accurate determination of the percolation exponent is most conveniently obtained from the temperature dependence of the longitudinal conductance at peak values. At temperatures of the order of the cyclotron gap ($k_BT \gtrsim \hbar\omega_c/4$), the maxima are washed out, so that the temperature dependence is then followed by working at constant B-field. The conductance peaks are studied in the breakdown regime at fields $B > B_c$, and are chosen such that the (unknown) temperature dependence of the spin gap does not play a role. Obviously, this puts a stringent constraint on the allowed peaks. The arrows in Fig. 2 indicate the peaks that we have analyzed in detail for sample 2.

The temperature dependences of the selected peaks are shown in Fig. 3 where a double logarithmic scale is used to better display the scaling laws. As reported for sample 1 in the main text, a minimum at the characteristic temperature scale $T^* = \hbar\omega_c/(4k_B)$ separating two temperature regimes with different scalings is seen for each studied peak in sample 2. This is again qualitatively consistent with formula (5). Note however, that in contrast to sample 1, the low temperature conductance peaks exceed the maximum value e^2/h (in the spin degenerate case) expected for a smooth potential [39, 28], see Fig. 3. Formula (5) is thus not appropriate to fit quantitatively the whole temperature range, as performed successfully with sample 1. We remind that formula (5) is derived for a smooth disorder potential characterized by a single length scale, an assumption which may not be totally correct for sample 2. Indeed the latter is a narrow quantum well with important surface roughness (and correspondingly lower

mobility), which is not accounted for in our model. We thus confine our study of the critical exponents to the high temperature regime above T^*, where density fluctuations are thermally smeared, so that equation (4) should still be valid in this regime. The resulting high-temperature longitudinal conductance is expressed as $\sigma_L = AT^{1-\kappa}$, where A is an amplitude dependent on magnetic field that will be taken as fit parameter. A second fit parameter is given by the critical exponent κ, and the results are compiled in Table 1.

B [T]	A [h/e^2 K$^{\kappa-1}$]	κ
2.2	0.47	0.84 ± 0.05
2.65	0.41	0.86 ± 0.05
3.23	0.36	0.89 ± 0.06

Table 1. Fit parameters for Fig. 3.

As a result, the extracted values for the exponent κ in sample 2 are still close to the theoretical prediction $\kappa \approx 0.77$, although we note here a slight overestimation. The systematic bias in κ observed in sample 2 could also be attributed to the more pronounced roughness of the disordered potential landscape compared to sample 1, as discussed above.

References

[1] K. von Klitzing, G. Dorda, and M. Pepper, Phys. Rev. Lett. **45**, 494 (1980).
[2] D. C. Tsui, H. L. Stormer, and A. C. Gossard Phys. Rev. Lett. **48**, 1559 (1982).
[3] T. Ando, A. B. Fowler, and F. Stern, Rev. Mod. Phys. **54**, 437 (1982).
[4] *The Quantum Hall Effect*, edited by R. E. Prange and S. M. Girvin (Springer, New York, 1987).
[5] M. Büttiker, Phys. Rev. B **38**, 9375 (1988).
[6] S. V. Iordansky, Solid State Commun. **43**, 1 (1982).
[7] R. F. Kazarinov and S. Luryi, Phys. Rev. B **25**, 7626 (1982).
[8] S. A. Trugman, Phys. Rev. B **27**, 7539 (1983).
[9] K. Hashimoto, C. Sohrmann, J. Wiebe, T. Inaoka, F. Meier, Y. Hirayama, R. A. Römer, R. Wiesendanger, and M. Morgenstern, Phys. Rev. Lett. **101**, 256802 (2008).
[10] K. Hashimoto, T. Champel, S. Florens, C. Sohrmann, J. Wiebe, Y. Hirayama, R. A. Römer, R. Wiesendanger, and M. Morgenstern, Phys. Rev. Lett. **109**, 116805 (2012).
[11] H. P. Wei, D. C. Tsui, M. A. Paalanen, and A. M. M. Pruisken, Phys. Rev. Lett. **61**, 1294 (1988).
[12] H. P. Wei, S. Y. Lin, and D. C. Tsui, and A. M. M. Pruisken, Phys. Rev. B **45**, 3926 (1992).
[13] W. Li, G. A. Csáthy, D. C. Tsui, L. N. Pfeiffer, and K. W. West, Phys. Rev. Lett. **94**, 206807 (2005).
[14] Y. J. Zhao, T. Tu, X. J. Hao, G. C. Guo, H. W. Jiang, and G. P. Guo, Phys. Rev. B **78**, 233301 (2008).
[15] W. Li, C. L. Vicente, J. S. Xia, W. Pan, D. C. Tsui, L. N. Pfeiffer, and K. W. West, Phys. Rev. Lett. **102**, 216801 (2009).
[16] W. Li, J. S. Xia, C. Vicente, N. S. Sullivan, W. Pan, D. C. Tsui, L. N. Pfeiffer, and K. W. West, Phys. Rev. B **81**, 033305 (2010).
[17] K. Saeed, N. A. Dodoo-Amoo, L. H. Li, S. P. Khanna, E. H. Linfield, A. G. Davies, and J. E. Cunningham, Phys. Rev. B **84**, 155324 (2011).
[18] J. T. Chalker and P. D. Coddington, J. Phys. C **21**, 2665 (1988).

[19] B. Huckestein, Rev. Mod. Phys. **67**, 357 (1995).
[20] B. M. Gammel and F. Evers, Phys. Rev. B **57**, 14829 (1998).
[21] P. Cain and R. A. Römer, Europhys. Lett. **66**, 104 (2004).
[22] B. Kramer, T. Ohtsuki, and S. Kettemann, Phys. Rep. **417**, 211 (2005).
[23] F. Evers and A. D. Mirlin, Rev. Mod. Phys. **80**, 1355 (2008).
[24] K. Slevin and T. Ohtsuki, Phys. Rev. B **80**, 041304(R) (2009).
[25] M. Amado, A. V. Malyshev, A. Sedrakyan, and F. Dominguez-Adame, Phys. Rev. Lett. **107**, 066402 (2011).
[26] H. Obuse, I. A. Gruzberg, and F. Evers, Phys. Rev. Lett. **109**, 206804 (2012).
[27] M. Flöser, S. Florens, and T. Champel, Phys. Rev. Lett. **107**, 176806 (2011).
[28] M. Flöser, S. Florens, and T. Champel, Int. J. Mod. Phys: Conf. Series **11**, 49 (2012).
[29] This sample was originally grown at Institute for Microstructural Sciences, National Research Council, Ottawa K1A 0R6, Canada.
[30] T. Rötger, G. J. C. L. Bruls, J. C. Maan, P. Wyder, K. Ploog, G. Wiemann, Phys. Rev. Lett. **62**, 90 (1989).
[31] A. M. Chang and D. C. Tsui, Solid State Commun. **56**, 153 (1985).
[32] H. Hirai, S. Komiyama, S. Sasa, and T. Fujii, Solid State Commun. **72**, 1033 (1989).
[33] V. Renard, Z. D. Kvon, G. M. Gusev, and J. C. Portal, Phys. Rev. B **70**, 033303 (2004).
[34] M. M. Fogler, A. Yu. Dobin, V. I. Perel, and B. I. Shklovskii, Phys. Rev. B **56**, 6823 (1997).
[35] D. G. Polyakov, F. Evers, A. D. Mirlin, and P. Wölfle, Phys. Rev. B **64**, 205306 (2001).
[36] I. M. Ruzin, Phys. Rev. B **47**, 15727 (1993).
[37] S. H. Simon and B. I. Halperin, Phys. Rev. Lett. **73**, 3278 (1994).
[38] D. G. Polyakov and B. I. Shklovskii, Phys. Rev. Lett. **74**, 150 (1995).
[39] A. M. Dykhne and I. M. Ruzin, Phys. Rev. B **50**, 2369 (1994).
[40] M. M. Fogler and B. I. Shklovskii, Sol. State Comm. **94**, 503 (1995).
[41] M. M. Fogler, D. G. Polyakov and B. I. Shklovskii, Surf. Sci. **361**, 255 (1996).
[42] H. L. Zhao and S. Feng, Phys. Rev. Lett. **70**, 4134 (1993).
[43] This derivation is close to the standard textbook version [44] of electron-phonon scattering, which has to be extended to take into account the Landau levels quantization.
[44] V. F. Gantmakher and Y. B. Levinson, *Carrier scattering in Metals and Semiconductors*, North-Holland, Amsterdam (1987).
[45] S. Iordanski and Y. Levinson, Phys. Rev. B **53**, 7308 (1996).